

RESEARCH ARTICLE

Natural gas facility methane emissions: measurements by tracer flux ratio in two US natural gas producing basins

Tara I. Yacovitch*, Conner Daube*, Timothy L. Vaughn[†], Clay S. Bell[†], Joseph R. Roscioli*, W. Berk Knighton[‡], David D. Nelson*, Daniel Zimmerle[†], Gabrielle Pétron^{§,||} and Scott C. Herndon*

Methane (CH₄) emission rates from a sample of natural gas facilities across industry sectors were quantified using the dual tracer flux ratio methodology. Measurements were conducted in study areas within the Fayetteville shale play, Arkansas (FV, Sept–Oct 2015, 53 facilities), and the Denver–Julesburg basin, Colorado, (DJ, Nov 2014, 21 facilities). Distributions of methane emission rates at facilities by type are computed and statistically compared with results that cover broader geographic regions in the US (Allen et al., 2013, Mitchell et al., 2015). DJ gathering station emission rates (kg CH₄ hr⁻¹) are lower, while FV gathering and production sites are statistically indistinguishable as compared to these multi-basin results. However, FV gathering station throughput-normalized emissions are statistically lower than multi-basin results (0.19% vs. 0.44%). This implies that the FV gathering sector is emitting less per unit of gas throughput than would be expected from the multi-basin distribution alone. The most common emission rate (i.e. mode of the distribution) for facilities in this study is 40 kg CH₄ hr⁻¹ for FV gathering stations, 1.0 kg CH₄ hr⁻¹ for FV production pads, and 11 kg CH₄ hr⁻¹ for DJ gathering stations. The importance of study design is discussed, including the benefits of site access and data sharing with industry and of a scientist dedicated to measurement coordination and site choice under evolving wind conditions.

Keywords: Oil and Gas; tracer release; dual tracer release; emission; methane; distributions

Introduction

Global atmospheric methane concentrations have increased in the past decade; however, attribution of the root causes has remained elusive (Turner et al., 2016; Rigby et al., 2017; Turner et al., 2017). With production of natural gas comes the potential for emissions of methane, its primary component. Emissions of this greenhouse gas have the potential to offset some of the climate benefit associated with switching from coal power plants to natural gas power plants. Emission rates of methane from the natural gas industry vary by both geographic region (Peischl et al., 2015) and industry sector (Allen et al., 2013; Mitchell et al., 2015; Subramanian et al., 2015). In this

study, we examine emission rates from different types of facilities across two natural gas extraction regions.

The natural gas supply chain is typically divided by industry sector. We focus here on the first four sectors: production, gathering, processing and transmission. Briefly, gas is extracted from the ground at wellpads (production sector: characteristic equipment includes wells and tanks for produced water or condensate). Multiple wellpads feed through a network of pipes into central gathering stations where gas is compressed (gathering sector: compressor houses, tank batteries, limited gas treatment equipment) and sent along to processing plants for separation of valuable non-methane hydrocarbons (NMHC) from the gas stream and for any remaining treatment of the natural gas (processing sector: distillation columns, turboexpanders, heat exchangers, etc.) Finally, the purified natural gas is sent to transmission stations (transmission sector: multiple large compressor houses) where it is pressurized further and sent via pipeline to be distributed and used.

Several recent studies have examined methane emissions in these four sectors of the natural gas industry. In a national production study, Allen et al. (2013) report measured methane emission rates from production sites in the US. Though the main results were based on engineering estimates and equipment-level measurements, the 2013

* Aerodyne Research, Inc. 45 Manning Road, Billerica, Massachusetts, US

[†] Energy Institute and Department of Mechanical Engineering, Colorado State University, Fort Collins, Colorado, 80524, US

[‡] Department of Chemistry and Biochemistry, Montana State University, Bozeman MT, 59717, US

[§] Cooperative Institute for Research in Environmental Sciences, University of Colorado Boulder, Boulder, Colorado, US

^{||} NOAA Earth System Research Laboratory, Boulder, Colorado, US

Corresponding author: Tara I. Yacovitch (tyacovitch@aerodyne.com)

study also published individual results from tracer flux ratio measurements downwind of 20 wellpads. These tracer results are explored in this manuscript. Subsequent studies published additional equipment-level emissions datasets for pneumatic controllers (Allen et al., 2015a) and liquid unloadings (Allen et al., 2015b). In a national gathering and processing study, Mitchell et al. (2015) used similar tracer methods to describe emission rate measurements from 114 gathering facilities and 16 processing plants across the US. They find skewed emissions distributions (“fat-tail” distributions), and that larger-throughput facilities have smaller throughput-normalized emissions. Subramanian et al. (2015) compared tracer release data to “bottom-up” summations of individual equipment leaks in a nation-wide study of the transmission and storage sector. These multi-basin studies paint a detailed picture of emission rates from these upstream sectors of the natural gas industry. Since they sampled from geographic regions across the US, they can serve as comparison datasets for facility-level emission rates from smaller geographic regions.

Basin-scale aircraft studies have shown that throughput-normalized emissions can vary significantly between regions. Peischl et al. (2015) report basin-level emission rates from three shale plays that make up over 50% of 2013 US gas production: the Haynesville (West Texas & Louisiana), Fayetteville (Arkansas) and Marcellus (Pennsylvania portion only) shale formations. They find that loss rates as a percentage of methane produced were lower than the previously studied Denver-Julesburg (Colorado) (Pétron et al., 2012; Pétron et al., 2014) and Uinta (Utah) plays (Karion et al., 2013).

This paper describes dual tracer flux ratio measurements (Roscioli et al., 2015) of methane emissions from oil and natural gas facilities. Tracer experiments involve releasing known amounts of tracer gases near to suspected methane emission locations. A mobile laboratory transects the resulting downwind enhancements of methane and tracer gases. The ratios of measured species’ mixing ratios, combined with known tracer release rate, determine emission rates. Such methods have been in use since the 1990’s (Lamb et al., 1995; Shorter et al., 1997), and unlike dispersion methods, tracer flux ratio measurements do not require knowledge of atmospheric stability and transport, and are independent of exact wind measurements and their timescales (Mønster et al., 2014; Roscioli et al., 2015). The use of two tracers allows for a self-contained quality check for each measurement (Allen et al., 2013; Roscioli et al., 2015).

The first study area sampled (DJ) was in the Denver-Julesburg oil and gas play in Colorado, US. This basin produces a combination of oil and gas. The gas is very rich in higher-hydrocarbons (C_2+ , meaning ethane and larger hydrocarbons), with molar ethane to methane ratios often in excess of 17% (see Supplemental Material (SM) Dataset S1). Benzene and other volatile organic hydrocarbons are also present. Methane emission rates from 12 gathering stations, 5 wellpads, and 4 processing plants were measured using tracer flux ratio methods during a 2-week period in November 2014. Though transmission lines

cross the region, no transmission-sector compressor stations were present within the study area.

The second study area (FV) was in the Fayetteville shale play, in Arkansas, US. The FV study area produces natural gas that is very low in C_2+ , with ethane to methane molar ratios <2% (see SM Dataset S1) or a very “dry gas” with no oil production. The gas is also “sweet”: absent of sulfur impurities like H_2S . These properties mean that very little processing is required before the gas is injected into the transmission system. The emission rates from 31 gathering stations, 18 wellpads and 4 transmission stations were measured by two mobile laboratories in a three-week period in September and October of 2015. No processing plants were present within the study area.

Both campaigns were performed under the umbrella of Research Partnership for a Secure Energy America (RPSEA). Additional results from these coordinated campaigns are published separately (Robertson et al., 2017; Schwietzke et al., 2017) including synthesis and reconciliation of diverse methodologies for the FV production sector (Bell et al., 2017) and the FV gathering sector (Vaughn et al., 2017).

Methane emission rates from wellpads, gathering stations, processing plants and transmission stations were quantified. The resulting distributions of emitters were compared to previous tracer flux ratio results from multi-basin studies (Allen et al., 2013; Mitchell et al., 2015; Subramanian et al., 2015). The distribution modes (i.e. most common emission rate) and widths (variability) were compared in order to assess whether each studied area was representative of the larger datasets.

Methods

The Aerodyne Mobile Laboratory (Kolb et al., 2004; Roscioli et al., 2015) (AML) step van and miniature AML (minAML) cargo van supported suites of meteorological and analytical equipment. Each vehicle was equipped with GPS and wind monitors and continuously sampled ambient air for methane (CH_4), ethane (C_2H_6), tracer release gases nitrous oxide (N_2O) and ethyne (C_2H_2), and other trace-gas species. Accompanying tracer release vehicles were equipped to transport, release and log tracer gas flows. Methane and tracer measurements were performed with Tunable Infrared Laser Direct Absorption Spectroscopy (TILDAS) trace-gas monitors from Aerodyne Research, Inc. with 1 second sub-ppb precisions of 0.10–0.30 ppb for CH_4 , 0.03–0.06 ppb for N_2O , and 0.03–0.10 ppb for C_2H_2 , depending on the laser region chosen. The full instrument suite is described in greater detail in SM Text S1, Section 1.

In planning these measurements, study coordinators divided the region into geographic clusters of sites (see SM Text S1, Section 2). The FV study area was divided into 17 clusters, 6 of which were chosen as primary measurement areas, in a 130 km by 60 km region. Gathering sites outside this 6-cluster focus area were also measured. The DJ study area was gridded into 12 separate clusters, in an 80 km by 76 km region.

Sampling typically occurred in a single cluster each day in coordination with the other study teams. Within the designated cluster, sites were chosen and visited depending on downwind road access based on the dominant

surface wind direction, and are expected to be representative of the larger study area's distributions of emitters. The exception to this rule is the set of wellpads measured in the DJ: higher-emitting sources flagged by collaborating teams were targeted for tracer flux ratio measurements.

Site access for the FV study was secured from operators comprising 82% of active production wells, 85% of midstream compression sites (gathering sector), and 67% of transmission sites. Escorts from one of these operators were assigned to each measurement group daily. Escorts did not know which region or set of sites would be sampled in advance. Besides restricting site choice to their company's assets, operators had no further influence on site choice. The DJ study was performed without site access, and tracer release positioning and measurements were restricted to public roads.

The tracer flux ratio method (sometimes "tracer release" or "tracer method") involves releasing known quantities of tracer gas(es) close to a suspected source at a facility (Lamb et al., 1995; Roscioli et al., 2015). In this study, N_2O and C_2H_2 were used as tracer gases to measure CH_4 emissions. These tracer gases were chosen because their ambient background concentrations are relatively constant; fast, high-precision instruments to measure them are available; and they are not expected to be present at oil and gas sites (with rare exceptions, see SM Text S1, Section 3).

Since downwind concentration enhancements are directly related to the flow rates at the source, the unknown methane flow (f_{CH_4} , in standard liters per minute, SLPM) was deduced based on the known tracer flow (f_{tracer} , SLPM) and the measured concentration enhancements (ΔCH_4 and $\Delta tracer$, in ppb):

$$f_{CH_4} = f_{tracer} \frac{\Delta CH_4}{\Delta tracer}$$

A major advantage of the tracer flux ratio method over other downwind techniques (Brantley et al., 2014; Thoma and Squier, 2014; Yacovitch et al., 2015) is that it requires no knowledge or simulation of atmospheric dispersion. Wind direction and speed are only used qualitatively, and no parameterization of atmospheric stability is required. Furthermore, placement of the tracers on or adjacent to a site allows the measured emissions to be attributed with certainty to that facility or even to a sub-section of the facility (Roscioli et al., 2015) depending on the proximity of the tracer to the emission source. To achieve this, downwind measurements were performed continuously while in motion to verify that the tracer gases and facility-associated CH_4 were enhanced above background over a similar spatial extent (see SM Text S1, Section 3). The ethane/methane enhancement ratio for each facility was also measured, and together with the spatial characteristics, allowed for methane emissions to be attributed to the site and for any interfering sources to be identified.

The strategies and results of tracer placement are discussed in detail by Roscioli et al. (2015). Briefly, the goal was to place release points as close to suspected methane emission points as possible, ideally closer than 20–50% of the downwind transect distance to the site

(Roscioli et al., 2015). Transects were then performed at downwind distances where all site emissions appear mixed; this also reduced concerns about missing emissions from elevated sources (SM Text S1, Section 4). On a wellpad, one tracer was typically placed next to the condensate/produced water tanks, and one next to the wellheads. At a mid-sized gathering station, one tracer was placed next to a bank of compressor houses, and the other next to a battery of condensate tanks. Very large facilities sometimes required performing two sets of experiments to quantify sub-sectors of the site. Tracers were occasionally moved partway through an experiment to better pinpoint an unexpected emission location. When no site access was available, tracers were released from the side of a public road. Ideally, release points bracketed a facility's fence line, however, in the DJ, facility size and private land restrictions usually prevented this ideal, and tracers were often simply released from an elevated point in the bed of a pickup-truck used as a release vehicle and parked at the facility fence line. Non-ideal tracer placement and road access were two factors that limited the quality of some acquired data and resulted in larger errors bar on the final facility emission rates.

For each facility, the AML or minAML measured a set of downwind plume transects. A plume transect is a section of data acquired downwind of a site by driving cross-wind (see the sample plume in SM Text S1, Section 3, or the tracer-only plume in **Figure 1**). It shows mixing ratios for methane, ethane and tracers going from background values, to elevated values and back again. It typically took the mobile laboratory 1–5 minutes to traverse a plume, and multiple transects were acquired for a given site over the course of 30 minutes to several hours. Several different methods for individual transect analysis were combined to yield the final average determination of the facility-level methane emission rate, in $kg CH_4 hr^{-1}$.

The measured ratio of tracers in the plume transect was divided by the known ratio of released tracer gases to get a "factor error" (see SM Text S1, Section 5). An automated algorithm determined the best analysis method based on this factor error and on R^2 values for the linear fits of mixing ratios pairs. Low-quality plumes were rejected in the process. The threshold values used were: $R^2 > 0.5$ and $0.5 < \text{factor error} < 2$. These choices aimed to balance the accuracy of each individual plume determination (high accuracy for fewer plumes) against the precision of the final site-wide average (higher precision via many replicates). SM Text S1, Section 5 explores different threshold choices.

The analysis methods chosen varied depending on acquisition distance, road geometry, size of the site and position of the tracers. These individual methods and the method choice algorithm were based upon Roscioli et al. (2015) and are described in SM Text S1, Section 5. In order of preference, the methods used were: 1) dual-tracer correlation, 2) single-tracer correlation, 3) area-area and 4) sum-sum. In non-ideal measurement situations, plumes were manually rejected or the method choice algorithm overridden. For example, if an emission source was further than expected from the tracers, tracer plumes would be

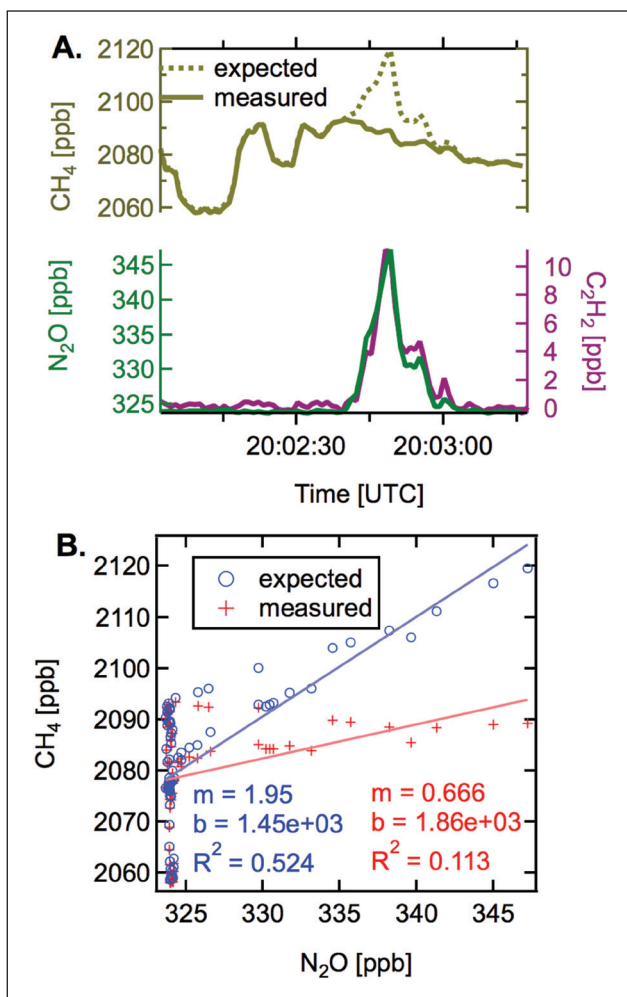


Figure 1: Method for determining the LOD_{TF} for the tracer flux ratio method. Panel A shows the measured N₂O and C₂H₂ tracers (solid green and solid purple) alongside the measured CH₄ (solid gold line) for this site with no detected CH₄ emissions. The expected CH₄ plume (dotted line, not real data) is also shown. Panel B (red crosses) shows the fit of measured CH₄ vs. N₂O data from Panel A and has a poor R². The fit of expected CH₄ vs. N₂O with R² ≥ 0.5 is shown (panel B, blue circles). DOI: <https://doi.org/10.1525/elementa.251.f1>

well correlated, but methane-tracer plumes would not. In this case, the area-area method would be manually chosen over the dual-tracer correlation method. Additional examples of exceptions to the algorithm are described in SM Text S1, Section 6.

The use of dual tracers released in known amounts allowed for a check of the data quality for each plume. The performance of the four analysis methods was evaluated by comparing the ratios of released to measured tracer (see SM Text S1, Section 7).

The final methane emission rate estimate for a particular facility was set to the arithmetic mean of all accepted plumes. The 95% confidence intervals on this emission rate were calculated from:

$$95\% \text{ CI} = t_{N-1}^{0.05} \cdot \frac{\sigma}{\sqrt{N}}$$

where $t_{N-1}^{0.05}$ is the two-sided Student's T at 95% confidence, N is the number of accepted plumes and σ is the standard deviation of methane emission rates for the accepted plumes, such that σ/\sqrt{N} is the standard error of the mean. This equation assumes that emission rates were constant with time during the experiment. Typically, N ranged between 5 and 10. In rare cases, only a single plume was accepted. For N = 1 results, the performance of the analysis method was used to estimate 95% confidence intervals (see SM Text S1, Section 7).

At three wellpads in the FV study area, tracer flux ratio methodology was used to quantify sites with no detected emissions, i.e. sites with emissions below the limit of detection for the tracer flux ratio method (LOD_{TF}). In these real-world measurement situations, the size of LOD_{TF} was not limited by instrument precision or instrument LOD (all <1 ppb and tabulated in SM Text S1, Section 1). Rather, variations in ambient methane on the order of 10–30 ppb during each downwind plume transect limited the ability to detect small concentration enhancements due to site emissions. Due to the influence of the local background, each LOD_{TF} is specific to a given site at a given measurement time and cannot be applied broadly across different sites. In the following paragraphs, we show an example of the empirical determination of the LOD_{TF} using real-world data.

The LOD_{TF} calculation was done for sites with clearly observed tracer concentration enhancements, but an absence of correlated methane signal (i.e. no detected methane emissions). A situation where neither tracer nor methane were observed would mean that the site was not actually being measured (a “fail”) and would not be appropriate for determination of the LOD_{TF}. This specific method was not developed for sites with detectable emissions (i.e. CH₄ enhancements correlated to a tracer) but analogous methodology could be devised.

A transect for a site in the FV dataset with no detected CH₄ plume was chosen with high-quality tracer signals. An example is shown in **Figure 1**, where the solid lines are the measured wet air mixing ratios of CH₄ (gold), N₂O (green) and C₂H₂ (purple). The correlation plot of CH₄ vs. N₂O is poor, with an R² of 0.113 (Panel B. red crosses). N₂O was chosen as the x-axis here since it had slightly better precision than C₂H₂; C₂H₂ could equally be used.

In the determination of LOD_{TF} a correlation plot was created by plotting a simulated “CH₄ expected” vs. the true measured N₂O. The expected methane trace is constructed as follows:

$$\text{CH}_4 \text{ expected} = \text{CH}_4 \text{ meas} + a \cdot (\Delta \text{N}_2\text{O meas}),$$

where CH₄ meas and N₂O meas are the measured trace-gas mixing ratios as a function of time, and $\Delta \text{N}_2\text{O meas}$ has been background corrected. The unitless factor *a* determines the size of the simulated CH₄ plume. In this procedure, *a* was increased from 0 in steps of 0.1 until the R² of the fit exceeded a threshold value, in this case an acceptance criteria of R² ≥ 0.5. The magnitude of R² was chosen to match the threshold value for the tracer flux ratio

analysis methods (SM Text S1, Section 5). In the example trace, the dotted line is the final CH_4 expected trace, with a factor of $a = 1.4$. This factor was then used along with the known N_2O flow rate (N_2O released, in SLPM) to determine the minimum CH_4 emission from the site that would be detected, or the LOD_{TF} (units of SLPM of CH_4):

$$\text{LOD}_{\text{TF}} = a \cdot \text{N}_2\text{O released.}$$

For this plume, with an N_2O release rate of 20 SLPM of N_2O , and including calibration factors, this method yielded a LOD_{TF} of 36 SLPM of CH_4 or, equivalently, $1.42 \text{ kg CH}_4 \text{ hr}^{-1}$.

This method assumes that any potential site methane emissions are co-located with the N_2O tracer, a good assumption as long as tracers were well-placed and transects were done far enough downwind (e.g. transects done at distances many times larger than the tracer – emission source distance). This procedure was repeated for each dual-tracer correlation plume, and the average of the LOD_{TF} 's was used as the upper 95% confidence limit for the final site emission.

In order to determine smaller LOD_{TF} 's and lower upper limits for these sites with no detected methane emissions, a combination of factors would be required: less baseline variation in CH_4 mixing ratio and better road access at intermediate distances downwind. These factors were typically fixed at a given site on any given day. However, measuring the same site under a different dominant wind direction would change road access and thus LOD_{TF} . Another way to reduce LOD_{TF} would be to perform multiple miniature dual tracer experiments on individual pieces of equipment, transecting the plume only tens of meters downwind while driving on facility property. Closer transects would result in smaller LOD_{TF} 's. Such LOD_{TF} minimization experiments were not attempted during this campaign, since the main goal was to do facility-scale measurements.

Results and discussion

Figure 2 shows final methane emission estimates in $\text{kg CH}_4 \text{ hr}^{-1}$ for all measured sites in the Fayetteville study area (FV, circles) and the Denver-Julesburg study area (DJ, triangles). Sites are ordered by sector, basin and emission rate. The data points are colored by sector, with production sites in red, gathering in green, transmission in blue, and processing in purple. No transmission stations were sampled in the DJ; no processing plants were present in the FV play. Error bars are reported at the 95% confidence level. Subsequent sections explore and contrast the distributions by sector; the lognormal mode from those comparisons is shown (grey lines) for distributions with sufficient numbers of data points to produce a fit: FV production, gathering and DJ gathering. The full dataset of emissions is available as a supplemental spreadsheet in SM Dataset S1 and partially reproduced in SM Text S1, Section 12.

General trends in emissions from the four sectors are evident in **Figure 2**. First, production sites (wellpads, red) have lower CH_4 emission rates than the other larger facilities in the transmission, gathering and processing sectors,

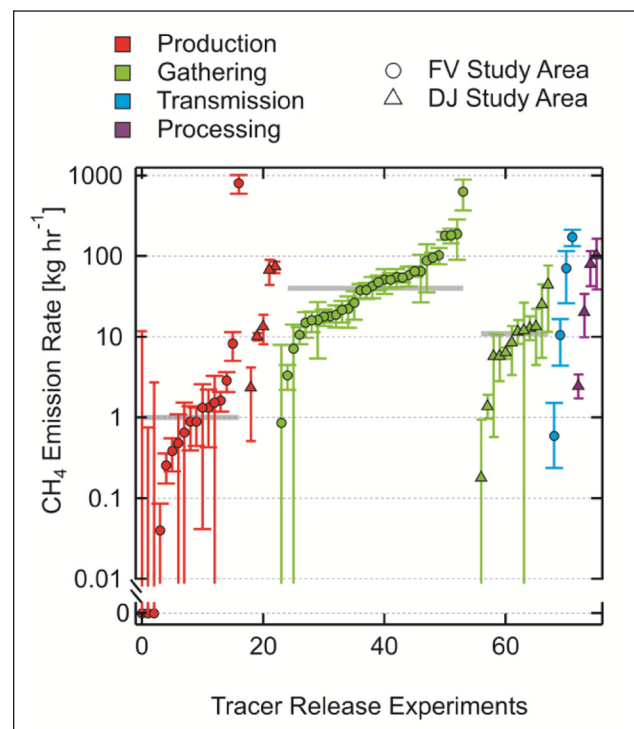


Figure 2: Measured methane emission rates with 95% confidence intervals. Facilities in the FV study area within the Fayetteville shale play (circles) and the DJ study area within the Denver-Julesburg basin (triangles) are shown. Points are colored by sector (red: production; green: gathering; blue: transmission and purple: processing). The most common emission rate (mode of a lognormal fit to the data) is shown for select distributions (grey lines). Sampling of these datasets was random, except for DJ wellpads (red triangles), which targeted high emitters. DOI: <https://doi.org/10.1525/elementa.251.f2>

with a few exceptions. Though the DJ wellpad emissions are higher than the FV wellpad emissions, they should not be directly compared due to the deliberate and directed sampling of high-emitting wellpads in the DJ study. The other DJ sectors do not have this same bias, and we see that the bulk of the DJ gathering station emission rates fall within similar orders of magnitude ($\sim 1\text{--}100 \text{ kg CH}_4 \text{ hr}^{-1}$) as the FV results, with a lower most common emission rate (mode, grey lines).

Three active sites in the FV had no detectable emissions via tracer release: wellpads 40, 41 and 51. These sites are shown below the axis break in **Figure 2**. The LOD_{TF} was determined individually for each valid dual-tracer correlation plume for each of these three sites (see methods section). The 95% upper confidence limit was then set as the average LOD_{TF} for each site. The resulting upper limits extend from $0.7\text{--}12 \text{ kg CH}_4 \text{ hr}^{-1}$, well within the range of most of other wellpad emissions. Other emissions with smaller rates were also successfully quantified. This illustrates the fact that these LOD_{TF} determinations are highly dependent on the specific measurement conditions (wind direction/speed and ensuing road access as well as ambient methane background variations). In fact, for two of

these sites, small enhancements of methane (~100 ppb) were measured directly downwind of the equipment when driving on the wellpad; however, at distances appropriate for the tracer flux ratio experiment (400–700 m for these two sites), these enhancements were not detectable above background variations in CH₄.

Campaign design had a large impact on the data from the DJ and FV plays. The DJ campaign was conducted without site access, and while driving on public roads. These restrictions severely limited the number of candidate sites and decreased the success rate of tracer flux ratio measurements. Issues associated with this approach have been discussed elsewhere (Goetz et al., 2015). In the DJ study area, except for rare examples, the tracer releases were not optimally co-located with a site's methane emissions. This precludes analysis via the preferred dual-tracer correlation method with the smallest expected error bars ($x_{-0.47x}^{+0.90x}$, where x is the emission rate, and error bars are not symmetric) and falls back on analysis via the area-area method with expanded method error bars of $x_{-0.59x}^{+3.09x}$ (see SM Text S1, Section 7). Low wind conditions during the 2-week DJ measurement campaign further limited the number of sites that could be sampled. In contrast, the FV campaign was conducted over a 3-week period with both site access and lease road access. Flexible site choice was allowed within sub-regions in order to adapt to changing wind directions day-to-day. Two mobile laboratories, tracer release vehicles and teams were also deployed. Overall, in the DJ basin, 25 sites (23 oil and gas sites) were attempted with tracer flux ratio, with 23 successful measurements (88% success rate). In the FV study area, 55 sites were attempted, with 52 successful measurements (94% success rate). Site access also required discussing the experimental plan with operators and addressing specific safety hazards at each location, leading to a longer setup time. Despite this, the sampling rate was only slightly lower in the FV vs. DJ: 2.5 sites/day/team in the FV vs. 2.8 sites/day/team in the DJ. Coordination efforts in the FV facilitated this rate, with an extra scientist managing daily site choice under evolving wind conditions.

Another characteristic that can be seen in **Figure 2** is the symmetry in the data when plotted on a logarithmic scale. Indeed, this indicates that the emission rates are not normally distributed around the mode. This was also seen in previous studies (Yacovitch et al., 2015; Zavala-Araiza et al., 2015; Brandt et al., 2016) including the multi-basin studies of the production, gathering, processing and transmission sectors (Allen et al., 2013; Mitchell et al., 2015; Subramanian et al., 2015). In order to better investigate and compare these measured distributions to the multi-basin studies, we compare histograms using statistical methods at 95% confidence. The data were binned in logarithmically increasing bin sizes, and each distribution was fit to a lognormal function $P(x)$:

$$P(x) = \frac{A}{\sigma\mu\sqrt{2\pi}} \exp\left\{-\frac{(\ln(x-\mu))^2}{2\sigma^2}\right\}.$$

The lognormal parameter μ determines the location of the distribution. The lognormal parameter σ gives the shape of the distribution and should not be confused with a standard deviation; a larger σ leads to a heavier tail and a more skewed distribution where the peak of the distribution is much less than the arithmetic mean. Parameter A is a normalization factor. The distributions were left un-normalized to visibly retain the differences in sample size between the multi-basin and this paper's results. For skewed distributions, the average does not give the most common emission. Instead, we considered the mode of the distribution, where the distribution peaks, which was calculated from:

$$\text{mode} = \exp(\mu - \sigma^2).$$

Figure 3 shows the results of the emission rate distributions from the FV study (gold) and from tracer release results published as part of recent multi-basin studies (Allen et al., 2013; Mitchell et al., 2015; Subramanian

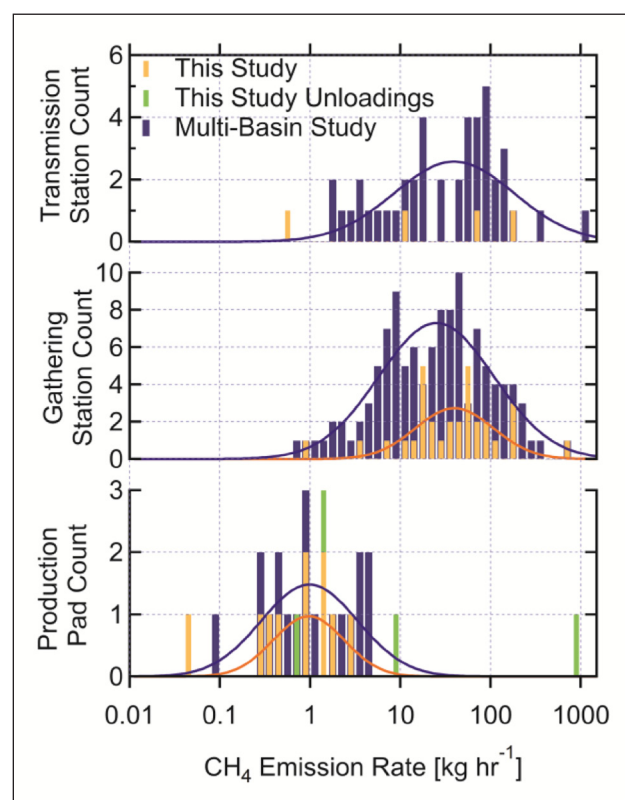


Figure 3: Comparison of the FV study region emission rates to multi-basin datasets. The blue distributions correspond to tracer flux ratio measurements from multi-basin studies by Allen et al. (2013) for production, Mitchell et al. (2015) for gathering and Subramanian et al. (2015) for transmission. The gold distributions correspond to the data from the FV study region within the Fayetteville Shale play. Fits were done to a lognormal distribution and coefficients are reproduced in SM Text S1, Section 9. Green bars show production facilities undergoing unloading at the time of operation and were excluded from the fits. DOI: <https://doi.org/10.1525/elementa.251.f3>

et al., 2015) (blue). The three wellpads from the FV with no detected emissions are not shown on these logarithmically scaled plots. The FV transmission sector distribution has only 4 data points, and so no clear distribution shape is evident. An analogous graph to **Figure 3** for the DJ study area is shown in SM Text S1, Section 8. The DJ dataset was too small to produce convincing distribution fits for most sectors; the deliberately skewed production sampling was also not appropriate for comparison.

Table 1 reports the emission rate results ($\text{kg CH}_4 \text{ hr}^{-1}$) from the distribution fits shown in **Figure 3**. The mode of the lognormal distribution is reported, and provides a quick comparison of emission rate magnitudes. The distribution widths are characterized by the 95% confidence intervals such that 95% of the area under the distribution curve is accounted for. The full set of lognormal fit parameters and their 1-sigma uncertainties are reported in SM Text S1, Section 9. These 1-sigma uncertainties were used to compare the emission distributions. The distributions were considered equivalent if the μ and σ parameters (lognormal location and shape) between different fits agreed to within twice their 1-sigma uncertainties, i.e. their $\pm 2 \cdot (1\text{-sigma uncertainty})$ error bars overlapped. An alternate method of comparison was also used: the Kolmogorov-Smirnov goodness-of-fit test (KS test) (Press et al., 1986), which probes whether a sample cumulative

distribution function could be drawn from a reference distribution at a given confidence level (95% is used here). The test is most sensitive near the center of the distribution and less sensitive to the tails. The benefit of this test is that it does not assume a given distribution shape.

In **Figure 3**, it is immediately evident that the production sector has lower facility-level emission rates than either the gathering or transmission sectors: $0.98\text{--}1.0 \text{ kg CH}_4 \text{ hr}^{-1}$ for production vs. $25\text{--}40 \text{ kg CH}_4 \text{ hr}^{-1}$ for transmission and gathering. This holds both at the multi-basin scale and for the FV study region. The transmission and gathering sectors show similar emission rates. Processing plants were not included in any of the distributions above, since the dry and sweet Fayetteville shale play does not require significant processing and no processing plants were within the defined study area boundaries. Results for the wet-gas DJ study area are shown in SM Text S1, Section 8, with gathering emission rates lower than the multi-basin results at $11 \text{ kg CH}_4 \text{ hr}^{-1}$ and sparse data in the production and processing sectors precluding distribution fits.

In comparing the production sector emission rates to previous results, we examine a few different datasets from the multi-basin study. First, we look at multi-basin data without regional distinctions. The multi-basin production study data from 19 tracer measurements are compared to

Table 1: Comparison of distributions between multi-basin results and the FV and DJ study areas. The mode of the lognormal distribution, 95% confidence interval (CI) as a measure of width and number of sites (N) are tabulated. DOI: <https://doi.org/10.1525/elementa.251.t1>

Sector	Distribution Characteristic	Multi-Basin: ^a Tracer Sites	FV Study Area	DJ Study Area	Multi-Basin: ^a Published Estimates
Emission Rate, in $\text{kg CH}_4 \text{ hr}^{-1}$					
Gathering	mode	25	40	11	
	width (95% CI)	12–3.3E3	15–7.3E2	4.5–75	
	N	115	33	12	
Production ^c	mode	0.98	1	n/a ^d	
	width (95% CI) ^b	0.39–48	0.36–12		
	N	19	10	5	
Throughput-Weighted Emissions, in %					
Gathering	mode	0.44	0.19	n/a	<1 ^e
	width (95% CI) ^b	12–3.3E3	0.08–0.77		
	N	115	31		
Production ^c	mode		~0.10 ^f		<0.42 ^g
	N		10		

^a Allen et al. (2013); Mitchell et al. (2015).

^b Widths are characterized by the 95% confidence interval (CI) for the distribution. See text.

^c FV production sites undergoing unloading are excluded.

^d Sampling of the DJ production sector was deliberately skewed, and thus no distribution statistics are reported.

^e Mitchell et al. (2015) report that 85 of 114 gathering sites had throughput-weighted emissions <1%.

^f Insufficient N to report data from distribution fit. Approximate mode is noted instead.

^g Allen et al. (2013) report production sector emissions, including unloadings, at 0.42% of gross gas production. FV results in this table deliberately exclude unloadings.

data from the FV study area. The lognormal fit parameters (SM Text S1, Section 9) for the FV production data are not statistically different from the multi-basin study, based on either 2-sigma error bars or the KS test. In these results, 4 sites undergoing unloading (manual and plunger unloadings, shown in green in **Figure 3**) were excluded from the statistical analysis. The three wellpads with no detected emissions did not contribute to the lognormal fit (lognormal scaling does not contain zero). The wellpad data are shown on a linear x-axis scale in SM Text S1, Section 9, but a lognormal fit of this data did not converge. However, the KS test is independent of any fitting algorithm and shows that the full production pad distribution is statistically indistinguishable from the multi-basin study. The regional breakdown of the tracer flux ratio dataset in **Figure 3** is available from the Allen et al. (2013) supplemental information. The data include 5 wellpad measurements in that study's mid-continental region, which includes the FV study region. These 5 wellpads are clustered at higher emission rates than the rest of the distribution, and are statistically different from this study's FV distribution of 17 wellpads (see SM Text S1, Section 10).

Concerns have been raised in recent years (Howard, 2015; Howard et al., 2015) over the validity of some Allen et al. (2013) results due to a failure mode of the Bacharach Hi-Flow Sampler used and due to possible biases in this same sensor for samples with high non-methane hydrocarbon (NMHC) content. These concerns have been examined and their implications analyzed elsewhere (Allen et al., 2015c; Alvarez et al., 2016). In the production pad comparisons shown in **Figure 1**, we look only at previous tracer flux ratio measurements; these data were also the only disaggregated results published (see the supplemental information for Allen et al., 2013). These tracer results do not include measurements made with the Bacharach sensor. In fact, all tracer and methane measurements examined in **Figure 1** were done using laser-based trace-gas spectrometers identical to or competitive with those described here (SM Text S1, Section 1). These high-precision spectrometers measured diluted ppm or ppb-level methane signals (vs. %-levels) and were neither exposed to nor affected by the same high levels of NMHC.

We note one particularly interesting point in the FV production data: wellpad 50 (**Figure 2**, red circle, top of graph) has an emission rate of $802 \pm 210 \text{ kg CH}_4 \text{ hr}^{-1}$, the largest emission rate measured in this study and nearly two orders of magnitude larger than any other wellpad measured in this basin. This site was measured during a manual unloading event vented directly to atmosphere, which lasted 4–8 hrs. Allen et al. (2013) measured 9 liquid unloading events as part of the 2013 study and 107 liquid unloadings in subsequent 2015 results (2015b); 12 of the latter are comparable to wellpad 50: manual unloadings without plungers from a region encompassing the FV study area. The emission rates during these 12 manual unloadings ranged from 125–1225 $\text{kg CH}_4 \text{ hr}^{-1}$, well above the bulk of the production sites under normal operation (see SM Text S1, Section 10). The emission from wellpad 50 of $802 \pm 210 \text{ kg CH}_4 \text{ hr}^{-1}$ falls near the top of this range. In fact, three other wellpads were undergoing unloading activities during these measurements: wellpads

38, 42 and 44. All three underwent plunger unloadings with low frequency (for example 1 unloading lasting 2 minutes once per hour). All 4 of these wellpads undergoing unloading were excluded from statistical analyses. Additional details about the annual count and average duration of these routine scheduled episodic events are included in the work of Bell et al. (2017), where emissions from unloadings are incorporated into final results.

The FV gathering sector has an emission rate distribution that is not different from the multi-basin gathering results (Mitchell et al., 2015) at 95% confidence using either the 2-sigma uncertainties for the lognormal fit parameters μ and σ or the KS test. This is despite different distribution peaks of $40 \text{ kg CH}_4 \text{ hr}^{-1}$ for the FV basin and $25 \text{ kg CH}_4 \text{ hr}^{-1}$ for the multi-basin study, and highlights the importance of using such statistical methods (see SM Text S1, Section 11 for regional breakdown). Interestingly, data for the DJ basin suggest that the gathering facility emission rate distribution is statistically different from multi-basin results, with a similar lognormal σ parameter but a significantly lower mode of $11 \text{ kg CH}_4 \text{ hr}^{-1}$ (see SM Text S1, Section 8).

The transmission sector in the FV basin includes 4 sites (67% of the basin's transmission stations). This sample size does not allow for a clear distribution to be drawn, but the data largely fall within the umbrella of the multi-basin emission rates. One site (site 16, emission of $0.59^{+0.92}_{-0.35} \text{ kg CH}_4 \text{ hr}^{-1}$, with asymmetric 95% confidence intervals as calculated in SM Text S1, Section 7) is lower than any of the multi-basin transmission sector sites: this site was not operational and compressors were depressurized (vented). In fact, all compressors at the second smallest-emitting transmission site (site 9, $10 \pm 6 \text{ kg CH}_4 \text{ hr}^{-1}$) were also depressurized. In these cases, methane emissions can come from leaky valves that isolate the site from the rest of the high-pressure transmission line. The multi-basin study (Subramanian et al., 2015) sampled sites that also span these operational states.

The distributions of emitters shown in **Figure 3** are lognormal in shape, with a heavy tail. In order to investigate this tail, we use the concept of a functional super-emitter (Zavala-Araiza et al., 2015): simply, a site that has a high emission compared to the facility throughput. Throughput data acquired from partner companies are available for a subset of sites from the FV study. From these results, a throughput-normalized emission was calculated, expressed in percent. These distributions are shown in **Figure 4**. Sites with no throughput information available are excluded from this plot. Site-specific gas composition, when available, was used to correct natural gas throughput to methane throughput. When not available, the median gas composition of all partner data was used (0.957 mol CH_4 per mol natural gas). Lognormal modes and distribution widths are reported in **Table 1**.

In **Figure 4** the FV gathering results yield a throughput-normalized emission distribution that is lognormal and peaked at 0.19%; this can be compared to 0.44% for the multi-basin study (Roscioli et al., 2015). There were too few production facilities measured, and with known throughput, to allow for a converged fit. Still, the FV production distribution peaks at around 0.10%, excluding all unloading sites shown in dark green. No site-by-site

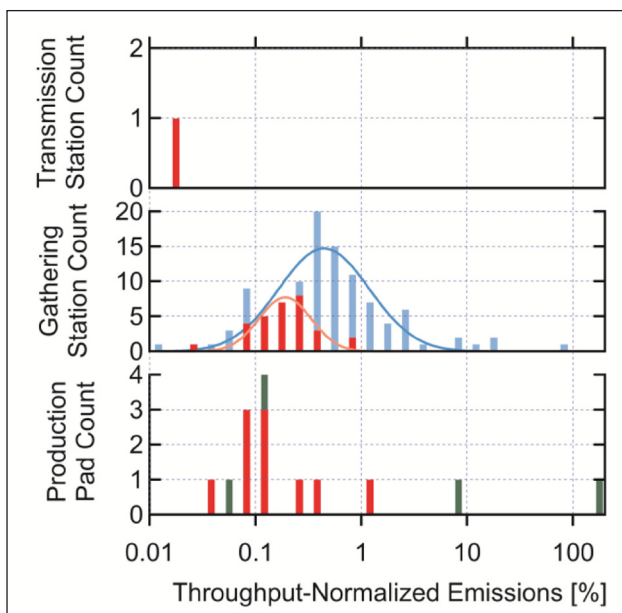


Figure 4: Throughput-normalized emission distributions. Production, gathering and transmission sectors in the FV basin (red) and for the multi-basin gathering sector (light blue) are compared. Production pads with unloadings (dark green) were excluded from the lognormal fits. DOI: <https://doi.org/10.1525/elementa.251.f4>

throughput data were published as part of the Allen et al. (2013) multi-basin study, precluding a direct comparison of distributions. However, they do report a final throughput-normalized emission of 0.42%, including unloadings. Excluding unloadings from the Allen et al. (2013) results would yield throughput-normalized emission rates $<0.42\%$, consistent with our 0.10% estimate.

The **Figure 4** production facility at $>100\%$ of throughput may be due to one or a combination of factors. 95% confidence limits on this particular data point are $\pm 40\%$ of throughput but alone are not enough to explain the discrepancy. The site's throughput on the measurement day may have been higher than the average over the course of the study period. Alternatively or additionally, the throughput for the unloading well that was vented to atmosphere may have been significantly higher than the same well when it was delivering to the pressurized gathering line at 200–275 kPa above ambient (~ 30 – 40 psig).

Throughput-normalized emission is not a good metric for the transmission sector. Transmission compressor stations are often turned off during seasonal lulls in natural gas demand (Subramanian et al., 2015). The pipelines they serve are kept pressurized, and the compressor houses may be pressurized or vented. Emissions are still possible from such sites, but a non-zero emission with zero throughput results in a calculated throughput-normalized emission that is infinite. Two such zero throughput sites in the FV basin were measured. A fourth transmission site has unknown throughput and therefore unknown throughput-normalized emissions.

While the distribution of methane emission rates in the FV gathering sector is not statistically different from the multi-basin study, the story changes when examining throughput-normalized emissions. FV gathering shows

significantly lower throughput-normalized emissions than the multi-basin study (0.19% vs 0.44%). This implies that the FV gathering sector is emitting less per unit of gas throughput than would be expected from multi-basin data alone. We leave to future studies any direct attribution of this lower proportional loss rate to basin characteristics such as wet/dry gas, type of equipment present, size of facilities and compressors, etc.

The most interesting aspect of these distributions is the difference in their shapes. The throughput-normalized emissions for FV gathering are lognormal in shape, as are the multi-basin gathering data. In contrast, the throughput-normalized emissions for FV production appear narrower and cannot be well fit by a lognormal function; this is likely due to the small number of sites included in the fit. Furthermore, while the two wellpads with highest throughput-normalized emissions were undergoing unloading, there are also two other unloading sites that fall within a similar percent range as wellpads that were not unloading. The tracer flux ratio experiment captures snapshots of the sites emissions, and so the duration and frequency of these plunger unloadings and their overlap in time with each individual downwind measurement will impact the final average emission rate. While these unloading sites were not included in any of the statistical analysis in this paper, such sites are important in understanding the overall emissions of the production sector and have been included in the results of Bell et al. (2017).

Summary

In this study, dual tracer flux ratio measurements of methane emission rates from oil and gas facilities were performed in two natural gas basins: the dry-gas Fayetteville Shale and the wet-gas Denver-Julesburg basin. A new method for empirical determination of the limits of detection for the tracer flux ratio method was developed, and demonstrated for three well pads with no detectable CH_4 emissions.

Representative sampling from the FV study area results in distributions of facility-level methane emission rates (in $\text{kg CH}_4 \text{ hr}^{-1}$) that are statistically indistinguishable from the previous multi-basin studies for both the gathering and production sectors. Transmission station results fall within the expected multi-basin distribution, except for a site that was decommissioned and vented with lower emissions. Conversely, when accounting for the amount of gas gathered at these sites, we find that the FV gathering sector has significantly lower throughput-normalized emissions than the multi-basin results.

Data are limited in the production sector both in number of FV study area measurements, and in throughput data for previous multi-basin results (Allen et al., 2013). As a result, we find no statistically significant difference in emission rates versus the multi-basin study and can make no statistical comparison of distributions with multi-basin throughput-normalized emissions.

Results from the DJ study area in the Denver-Julesburg basin show a gathering emission rate distribution that is statistically different in magnitude (lower) than the multi-basin study, but lack of throughput data

precludes additional comparisons. The differences in data availability between the FV and DJ studies highlight the benefits of the FV study experimental design. Site access and flexible site choice lead to improved data quality (including reduced error bars), higher site quantification success rate, known gas throughput, and other inside knowledge about site operations and equipment.

Data Accessibility Statement

Site IDs, sectors, methane emission rates with error bars, ethane/methane ratios with error bars and plume durations are uploaded as SM Dataset S1 in Microsoft Excel .xlsx format.

Supplemental Files

The supplemental files for this article can be found as follows:

- **Text S1.** Supplemental discussion, containing Sections 1 through 12 (PDF file). DOI: <https://doi.org/10.1525/elementa.251.s1>
- **Dataset S1.** Site emissions dataset for the FV and DJ study areas (Microsoft Excel .xlsx file). DOI: <https://doi.org/10.1525/elementa.251.s2>

Acknowledgements

We acknowledge the study funders who also provided operational data and/or site access. Additional data and/or site access were also provided by CenterPoint, Enable Midstream Partners, Kinder Morgan, and BHP Billiton.

Funding information

Funding for this work was provided by RPSEA/NETL contract no 12122-95/DE-AC26-07NT42677 to the Colorado School of Mines. Cost share for this project was provided by Colorado Energy Research Collaboratory, the National Oceanic and Atmospheric Administration, Southwestern Energy, XTO Energy, a subsidiary of ExxonMobil, Chevron, Statoil and the American Gas Association.

Competing interests

The authors have no competing interests to declare.

Author contributions

- Substantial contributions to conception and design: TIY, TLV, CSB, DZ, GP, SCH
- Acquisition of data: TIY, CD, TLV, CSB, JRR, WBK, SCH
- Analysis and interpretation of data: TIY, CD, JRR, DDN, SCH
- Drafted the manuscript and/or revised it critically: TIY, CD, TLV, CSB, JRR, DZ, GP, SCH
- Approved the submitted version for publication: all authors

References

Allen, DT, Pacsi, AP, Sullivan, DW, Zavala-Araiza, D, Harrison, M, et al. 2015a Methane emissions from process equipment at natural gas production sites in the United States: Pneumatic controllers. *Environ*

Sci Technol **49**(1): 633–640. DOI: <https://doi.org/10.1021/es5040156>

Allen, DT, Sullivan, DW and Harrison, M 2015c Response to comment on “methane emissions from process equipment at natural gas production sites in the United States: Pneumatic controllers”. *Environ Sci Technol* **49**(6): 3983–3984. DOI: <https://doi.org/10.1021/acs.est.5b00941>

Allen, DT, Sullivan, DW, Zavala-Araiza, D, Pacsi, AP, Harrison, M, et al. 2015b Methane emissions from process equipment at natural gas production sites in the United States: Liquid unloadings. *Environ Sci Technol* **49**(1): 641–648. DOI: <https://doi.org/10.1021/es504016r>

Allen, DT, Torres, VM, Thomas, J, Sullivan, DW, Harrison, M, et al. 2013 Measurements of methane emissions at natural gas production sites in the United States. *Proc Natl Acad Sci U S A* **110**(44): 17768–17773. DOI: <https://doi.org/10.1073/pnas.1304880110>

Alvarez, RA, Lyon, DR, Marchese, AJ and Robinson, AL, Hamburg, SP 2016 Possible malfunction in widely used methane sampler deserves attention but poses limited implications for supply chain emission estimates. *Elem Sci Anth* **4**: 137. DOI: <https://doi.org/10.12952/journal.elementa.000137>

Bell, CS, Vaughn, TL, Zimmerle, D, Scott, CH, Yacovitch, TI, et al. 2017 Comparison of methane emission estimates from multiple measurement techniques at natural gas production pads. *Elem Sci Anth*. In press. DOI: <https://doi.org/10.1525/elementa.266>

Brandt, AR, Heath, GA and Cooley, D 2016 Methane leaks from natural gas systems follow extreme distributions. *Environ Sci Technol* **50**(22): 12512–12520. DOI: <https://doi.org/10.1021/acs.est.6b04303>

Brantley, HL, Thoma, ED, Squier, WC, Guven, BB and Lyon, D 2014 Assessment of methane emissions from oil and gas production pads using mobile measurements. *Environ Sci Technol* **48**(24): 14508–14515. DOI: <https://doi.org/10.1021/es503070q>

Goetz, JD, Floerchinger, C, Fortner, EC, Wormhoudt, J, Massoli, P, et al. 2015 Atmospheric emission characterization of Marcellus Shale natural gas development sites. *Environ Sci Technol* **49**(11): 7012–7020. DOI: <https://doi.org/10.1021/acs.est.5b00452>

Howard, T 2015 University of Texas study underestimates national methane emissions at natural gas production sites due to instrument sensor failure. *Energy Sci Eng* **3**(5): 443–455. DOI: <https://doi.org/10.1002/ese3.81>

Howard, T, Ferrara, TW and Townsend-Small, A 2015 Sensor transition failure in the high flow sampler: Implications for methane emission inventories of natural gas infrastructure. *J Air Waste Manage Assoc* **65**(7): 856–862. DOI: <https://doi.org/10.1080/10962247.2015.1025925>

- Karion, A, Sweeney, C, Pétron, G, Frost, G, Michael Hardesty, R**, et al. 2013 Methane emissions estimate from airborne measurements over a western United States natural gas field. *Geophys Res Lett* **40**(16): 4393–4397. DOI: <https://doi.org/10.1002/grl.50811>
- Kolb, CE, Herndon, SC, McManus, JB, Shorter, JH, Zahniser, MS**, et al. 2004 Mobile laboratory with rapid response instruments for real-time measurements of urban and regional trace gas and particulate distributions and emission source characteristics. *Environ Sci Technol* **38**: 5694–5703. DOI: <https://doi.org/10.1021/es030718p>
- Lamb, BK, McManus, JB, Shorter, JH, Kolb, CE, Mosher, B**, et al. 1995 Development of atmospheric tracer methods to measure methane emissions from natural-gas facilities and urban areas. *Environ Sci Technol* **29**(6): 1468–1479. DOI: <https://doi.org/10.1021/es00006a007>
- Mitchell, AL, Tkacik, DS, Roscioli, JR, Herndon, SC, Yacovitch, TI**, et al. 2015 Measurements of methane emissions from natural gas gathering facilities and processing plants: Measurement results. *Environ Sci Technol* **49**(5): 3219–3227. DOI: <https://doi.org/10.1021/es5052809>
- Mønster, JG, Samuelsson, J, Kjeldsen, P, Rella, CW and Scheutz, C** 2014 Quantifying methane emission from fugitive sources by combining tracer release and downwind measurements – a sensitivity analysis based on multiple field surveys. *Waste Manag* **34**(8): 1416–1428. DOI: <https://doi.org/10.1016/j.wasman.2014.03.025>
- Peischl, J, Ryerson, TB, Aikin, KC, de Gouw, JA, Gilman, JB**, et al. 2015 Quantifying atmospheric methane emissions from the Haynesville, Fayetteville, and northeastern Marcellus shale gas production regions. *J Geophys Res, [Atmos]* **120**(5): 2119–2139. DOI: <https://doi.org/10.1002/2014JD022697>
- Pétron, G, Frost, G, Miller, BR, Hirsch, AI, Montzka, SA**, et al. 2012 Hydrocarbon emissions characterization in the Colorado Front Range: A pilot study. *J Geophys Res, [Atmos]* **117**(D4): D04304. DOI: <https://doi.org/10.1029/2011JD016360>
- Pétron, G, Karion, A, Sweeney, C, Miller, BR, Montzka, SA**, et al. 2014 A new look at methane and nonmethane hydrocarbon emissions from oil and natural gas operations in the Colorado Denver-Julesburg basin. *J Geophys Res, [Atmos]* **119**(11): 6836–6852. DOI: <https://doi.org/10.1002/2013JD021272>
- Press, WH, Flannery, BP, Teukolsky, SA and Vetterling, WT** 1986 Kolmogorov-Smirnov test. *Numerical recipes*. New York: Cambridge University Press: 818.
- Rigby, M, Montzka, SA, Prinn, RG, White, JWC, Young, D**, et al. 2017 Role of atmospheric oxidation in recent methane growth. *Proc Nat Acad Sci* **114**(21): 5373–5377. DOI: <https://doi.org/10.1073/pnas.1616426114>
- Robertson, AM, Edie, R, Snare, D, Soltis, J, Field, RA**, et al. 2017 Variation in methane emission rates from well pads in four oil and gas basins with contrasting production volumes and compositions. *Environ Sci Technol* **51**(15): 8832–8840. DOI: <https://doi.org/10.1021/acs.est.7b00571>
- Roscioli, JR, Yacovitch, TI, Floerchinger, C, Mitchell, AL, Tkacik, DS**, et al. 2015 Measurements of methane emissions from natural gas gathering facilities and processing plants: Measurement methods. *Atmos Meas Tech* **8**(5): 2017–2035. DOI: <https://doi.org/10.5194/amt-8-2017-2015>
- Schwietzke, S, Pétron, G, Conley, S, Pickering, C, Mielke-Maday, I**, et al. 2017 Improved mechanistic understanding of natural gas methane emissions from spatially resolved aircraft measurements. *Environ Sci Technol* **51**(12): 7286–7294. DOI: <https://doi.org/10.1021/acs.est.7b01810>
- Shorter, JH, McManus, JB, Kolb, CE, Allwine, EJ, Siverson, R**, et al. 1997 Collection of leakage statistics in the natural gas system by tracer methods. *Environ Sci Technol* **31**(7): 2012–2019. DOI: <https://doi.org/10.1021/es9608095>
- Subramanian, R, Williams, LL, Vaughn, TL, Zimmerle, D, Roscioli, JR**, et al. 2015 Methane emissions from natural gas compressor stations in the transmission and storage sector: Measurements and comparisons with the EPA greenhouse gas reporting program protocol. *Environ Sci Technol* **49**(5): 3252–3261. DOI: <https://doi.org/10.1021/es5060258>
- Thoma, E and Squier, B** 2014 OTM 33 geospatial measurement of air pollution, remote emissions quantification (gmap-req) and OTM33A geospatial measurement of air pollution-remote emissions quantification-direct assessment (GMAP-REQ-DA). Available at: https://cfpub.epa.gov/si/si_public_record_report.cfm?dirEntryId=309632.
- Turner, AJ, Frankenberg, C, Wennberg, PO and Jacob, DJ** 2017 Ambiguity in the causes for decadal trends in atmospheric methane and hydroxyl. *Proc Nat Acad Sci* **114**(21): 5367–5372. DOI: <https://doi.org/10.1073/pnas.1616020114>
- Turner, AJ, Jacob, DJ, Benmergui, J, Wofsy, SC, Maasakkers, JD**, et al. 2016 A large increase in U.S. Methane emissions over the past decade inferred from satellite data and surface observations. *Geophys Res Lett* **43**(5): 2218–2224. DOI: <https://doi.org/10.1002/2016GL067987>
- Vaughn, TL, Bell, CS, Yacovitch, TI, Roscioli, JR, Herndon, SC**, et al. 2017 Comparing facility-level methane emission rate estimates at natural gas gathering and boosting stations. *Elem Sci Anth*. In press. DOI: <https://doi.org/10.1525/elementa.257>
- Yacovitch, TI, Herndon, SC, Pétron, G, Kofler, J, Lyon, D**, et al. 2015 Mobile laboratory observations of methane emissions in the Barnett Shale region. *Environ Sci Technol* **49**(13): 7889–7895. DOI: <https://doi.org/10.1021/es506352j>
- Zavala-Araiza, D, Lyon, D, Alvarez, RA, Palacios, V, Harriss, R**, et al. 2015 Toward a functional definition of methane super-emitters: Application to natural gas production sites. *Environ Sci Technol* **49**(13): 8167–8174. DOI: <https://doi.org/10.1021/acs.est.5b00133>

How to cite this article: Yacovitch, TI, Daube, C, Vaughn, TL, Bell, CS, Roscioli, JR, Knighton, WB, Nelson, DD, Zimmerle, D, Pétron, G and Herndon, SC 2017 Natural gas facility methane emissions: measurements by tracer flux ratio in two US natural gas producing basins. *Elem Sci Anth*, 5: 69. DOI: <https://doi.org/10.1525/elementa.251>

Domain Editor-in-Chief: Detlev Helmig, Institute of Alpine and Arctic Research, University of Colorado Boulder, US

Associate Editor: Isobel Jane Simpson, Department of Chemistry, University of California, Irvine, US

Knowledge Domain: Atmospheric Science

Part of an *Elementa* Forum: Oil and Natural Gas Development: Air Quality, Climate Science, and Policy

Submitted: 12 May 2017 **Accepted:** 28 September 2017 **Published:** 24 November 2017

Copyright: © 2017 The Author(s). This is an open-access article distributed under the terms of the Creative Commons Attribution 4.0 International License (CC-BY 4.0), which permits unrestricted use, distribution, and reproduction in any medium, provided the original author and source are credited. See <http://creativecommons.org/licenses/by/4.0/>.



Elem Sci Anth is a peer-reviewed open access journal published by University of California Press.

OPEN ACCESS 